iScience

CellPress
OPEN ACCESS

Article

CKR-1 orchestrates two motor states from a single motoneuron in *C. elegans*

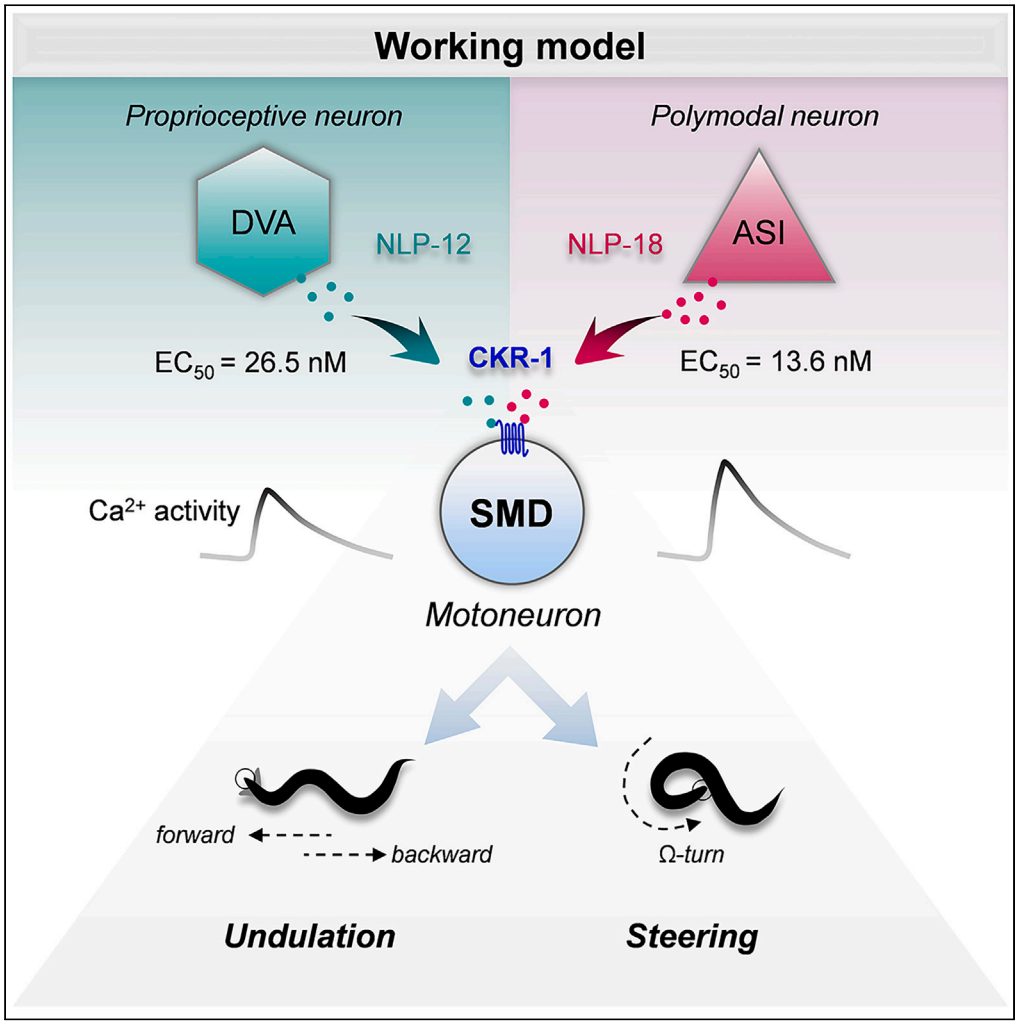

Lili Chen, Pan Su, Ya Wang, Yuting Liu, Li-Ming Chen, Shangbang Gao

sgao@hust.edu.cn

Highlights

CKR-1 modulates body bending and head steering through NLP-12 and NLP-18, respectively

CKR-1 signaling is dispensable for neurotransmission at the *C. elegans* NMJ

CKR-1 functions within a single head motor neuron, SMD

CKR-1 displays distinct sensitivities to NLP-12 and NLP-18

Chen et al., iScience *27*, 109390
April 19, 2024
https://doi.org/10.1016/j.isci.2024.109390

iScience

CellPress
OPEN ACCESS

Article

CKR-1 orchestrates two motor states from a single motoneuron in *C. elegans*

Lili Chen,[1,3] Pan Su,[1,2,3] Ya Wang,[1,3] Yuting Liu,[1] Li-Ming Chen,[1] and Shangbang Gao[1,4,*]

SUMMARY

Neuromodulation is pivotal in modifying neuronal properties and motor states. CKR-1, a homolog of the cholecystokinin receptor, modulates robust escape steering and undulation body bending in *C. elegans*. Nevertheless, the mechanisms through which CKR-1 governs these motor states remain elusive. We elucidate the head motoneuron SMD as the orchestrator of both motor states. This regulation involves two neuropeptides: NLP-12 from DVA enhances undulation body curvature, while NLP-18 from ASI amplifies Ω-turn head curvature. Moreover, synthetic NLP-12 and NLP-18 peptides elicit CKR-1-dependent currents in *Xenopus* oocytes and Ca^{2+} transients in SMD neurons. Notably, CKR-1 shows higher sensitivity to NLP-18 compared to NLP-12. *In situ* patch-clamp recordings reveal CKR-1, NLP-12, and NLP-18 are not essential for neurotransmission at *C. elegans* neuromuscular junction, suggesting that SMD independently regulates head and body bending. Our studies illustrate that a single motoneuron SMD utilizes a cholecystokinin receptor CKR-1 to integrate two motor states.

INTRODUCTION

Neuromodulation, a fundamental process in the nervous system, plays a pivotal role in shaping neuronal properties, which, in turn, influences diverse behavioral outputs, especially in the context of motor behaviors.[1–5] The dynamic regulation of neuronal functions by neuromodulatory signals is crucial for the adaptability and plasticity of neural circuits.[6] It enables the nervous system to fine-tune its responses to varying internal and external stimuli, leading to a wide range of behavioral outcomes. In motor behaviors, neuromodulation has emerged as a critical determinant in shaping movement patterns, motor coordination, and locomotion.[1,7–9] Dysregulation of precise neuromodulatory control leads to various motor disorders.[10,11]

Neuropeptides, which represent a vast and chemically diverse set of neuromodulators, impact various aspects of neural processing via activation of their cognate receptors.[12–14] To elucidate the significance of neuromodulation in neuronal and behavioral regulation, extensive investigations on neuropeptide receptors have been performed in various model systems, including *Caenorhabditis elegans*, *Drosophila*, rodents, and primates.[13,15–18] Nematode *C. elegans* genome predicts 115 proneuropeptide and more than 1,000 neuropeptide receptor genes,[12,13] providing a great genetic model to study the diversity and essential function of neuromodulation. Disruption of their signaling pathways in *C. elegans* leads to serious behavioral defects.[7,8] In general, neuropeptides typically activate specific neuropeptide receptors to regulate distinct behaviors. Interestingly, the capacity of a single neuropeptide receptor to be activated by multiple neuropeptides has been commonly observed in both *in vivo* and *in vitro* studies,[19,20] raising a compelling question about how these receptors receive and integrate information from diverse neuropeptides. The existence of receptor functional diversity challenges our understanding of the complexity and specificity of neuropeptide signaling in neural circuits. Elucidating the underlying mechanisms is essential to comprehend the fine-tuned and context-dependent regulation of neural activity and behavior.

In response to noxious stimuli, most of *C. elegans* exhibit robust a three-step escape motor response: reversal, full omega (Ω) turn, and forward with a different heading angle. Full omega (Ω) turn was defined the head bends toward the ventral body then sliding along the posterior of body after touch. This strategy of escape generate a greater escape angle to efficient escape. The full omega turn allows *C. elegans* to escape danger at the largest possible angle. We recently identified that a cholecystokinin (CCK) receptor, CKR-1, a $G\alpha_q$-protein-coupled receptor (GPCR), forms an essential signaling pathway for full omega (Ω) turn during escape steering.[21] A previously functionally unknown neuropeptide, NLP-18, was found to activate CKR-1 and enable the escape circuit to execute the full turn. NLP-18 is mainly secreted by the gustatory sensory neuron ASI to activate CKR-1 in the head motor neuron SMD and the turn-initiating interneuron AIB.[21] Meanwhile, another neuropeptide NLP-12 was identified to activate CKR-1 and CKR-2, the predicted second cholecystokinin receptor in *C. elegans*.[1,7]

[1]Key Laboratory of Molecular Biophysics of the Ministry of Education, College of Life Science and Technology, Huazhong University of Science and Technology, Wuhan 430074, China
[2]Present address: Henan Collaborative Innovation Center for Research and Development on the Whole Industry Chain of Yu-Yao, Henan Key Laboratory for Modern Research on Zhongjing's Herbal Formulae, Academy of Chinese Medical Sciences, Henan University of Chinese Medicine, Zhengzhou 450046, China
[3]These authors contributed equally
[4]Lead contact
*Correspondence: sgao@hust.edu.cn
https://doi.org/10.1016/j.isci.2024.109390

NLP-12 was originally identified as a secretion of a stretch-activated mechanosensory neuron DVA.[8] It mediates proprioceptive feedback, linking muscle contraction to changes in presynaptic release through the activation of CKR-2 in excitatory motor neurons.[8,22] Interestingly, during local food searching, NLP-12 acts primarily through CKR-1 in SMD motoneuron to enhance body bending.[7] An essential question arises: how does CKR-1 in a single head motoneuron, SMD, perceive the two neuropeptides, NLP-18 and NLP-12, to coordinate the motor actions of head steering and body bending?

In this study, we investigated the dual modulations of CKR-1 in two motor states: escape head steering and undulation body bending. By quantitative behavior analysis, we found that NLP-18 and NLP-12 independently modify the curvatures of the two motor states, which were both disrupted in *ckr-1* mutants. When CKR-1 is specifically knocked out in SMD neurons, the animals replicate the body curvature and Ω curvature defects observed in *ckr-1* mutants. However, when CKR-1 is knocked out in AIB neurons, it only reduces Ω curvature. More intriguingly, reciprocal cross-expression of NLP-18 in DVA in the *nlp-12* mutant or NLP-12 in ASI in the *nlp-18* mutant fails to restore their respective regulated curvatures. *In situ* electrophysiology and Ca^{2+} imaging, as well as *in vitro* oocyte expression experiment, further revealed that NLP-18 showed a modest higher affinity for CKR-1 than NLP-12, and they did not appear to directly regulate motor neuron activity. Hence, our findings demonstrate that the neuropeptide receptor CKR-1, with its differential sensitivity to neuropeptides, orchestrates two distinct motor states from a single motoneuron in *C. elegans*.

RESULTS

ckr-1 modulates two motor states: head steering and undulation body bending

To investigate how CKR-1 coordinates the motor actions of head steering and body bending, we conducted a detailed examination of the body curvature in the well-fed free-moving nematode *C. elegans* during forward and backward locomotion. Forward and backward motor states are characterized by continuous sinusoidal undulation of the body, referred to as undulation body bending (Figure 1A). Additionally, the nematode exhibits escape behavior, initiated either spontaneously or in response to head stimulation, wherein it first reverses and then executes a head steering behavior (omega turn or Ω-turn) to change its direction of movement (Figure 1A). In order to explore the neuromodulation mechanism on body bending and head Ω-turn steering, we quantified the "body curvature" from head to tail during forward and backward, respectively (Figure 1Bi), as well as the head steering "Ω curvature" in the anterior part of the body (0%–60%) (Figure 1Bii). This comprehensive analysis allowed us to gain insights into the coordination of these distinct motor states by CKR-1.

To explore the potential dual role of CKR-1 in multiple motor states, we quantified the aforementioned curvatures in these two movement states. Compared to the wild-type animals, *ckr-1* mutants revealed significant alterations in both motor states: (1) A noticeable reduction in body curvature during forward and backward movements (Figures 1Ci and 1Di) and (2) A significant decrease in head Ω curvature during escape behavior (Figures 1Cii and 1Dii). CKR-2 and CKR-1 are both GPCRs that share similarity with vertebrate CCKR GPCRs.[23] However, their expression patterns largely do not overlap.[8,21] This suggests that CKR-2 and CKR-1 may serve distinct roles in modulating behaviors. Indeed, we found that, unlike CKR-1, which is required for both motor states, the absence of CKR-2 only disrupts body curvature, while Ω curvature remains at wild-type levels (Figure S1). In addition, the removal of both CKR-1 and CKR-2 (*ckr-1; ckr-2*) recapitulated the defects observed in the *ckr-1* mutant (Figure S1). This suggests that, in contrast to CKR-1, CKR-2 appears to specifically function in regulating body bending.

These findings provide strong evidence for the involvement of CKR-1 in the modulation of two distinct motor states: escape head steering and undulation body bending.

NLP-12 and NLP-18 independently regulate body bending and head steering

Despite the impairment of both distinct motor states in the *ckr-1* mutant, it is worth noting that the parameters we analyzed are related to the curvature of the body, albeit in slightly different locations. This raises the question of whether CKR-1's regulatory role is derived from a common function in both head steering and undulation body bending. In other words, can these two motor behaviors be independently modulated? To investigate this, we employed mutants for *nlp-12* and *nlp-18*, which encode two distinct neuropeptides capable of activating CKR-1.[8,21]

NLP-12, a homolog of mammalian CCK, has been shown to regulate proprioceptive feedback and body bending amplitude in previous studies.[1,7,8] These regulatory effects are largely mediated through the activation of both CKR-1 and CKR-2, the second CCK receptor homolog in *C. elegans*.[8] In light of these findings, we further investigated the role of NLP-12 in modulating body curvatures, and also explored whether NLP-12, similar to CKR-1, could regulate Ω curvature during head steering. Consistent with its role in body bending regulation, we observed that in *nlp-12* mutants, the undulation body curvature was attenuated during both forward and backward locomotion (Figure 1Di). However, the Ω curvature during escape steering in *nlp-12* was comparable to that of the wild-type animals (Figure 1Dii). This result suggests that NLP-12's regulatory function is specifically targets undulation body bending, while it does not have a significant impact on head steering.

NLP-18, a nematode peptide containing the characteristic C-terminal residues "FAFA" or "FA,"[12,21] has been previously shown to regulate the Ω curvature during escape steering by activating CKR-1.[21] Given its role in head steering modulation, we investigated whether NLP-18 could also affect body bending, similar to CKR-1. Surprisingly, our findings revealed that the body curvature in *nlp-18* mutants remained unaffected during both forward and backward locomotion (Figure 1Di). In contrast, we observed a clear impairment in head curvature during Ω-turn (Figure 1Dii), indicating that NLP-18 specifically modulates head steering but does not influence body bending.

These findings shed light on the distinct roles of NLP-12 and NLP-18 in modulating different motor behaviors in *C. elegans*. NLP-12 appears to be specialized in regulating undulation body bending, while NLP-18 is only involved in head steering. The specificity of

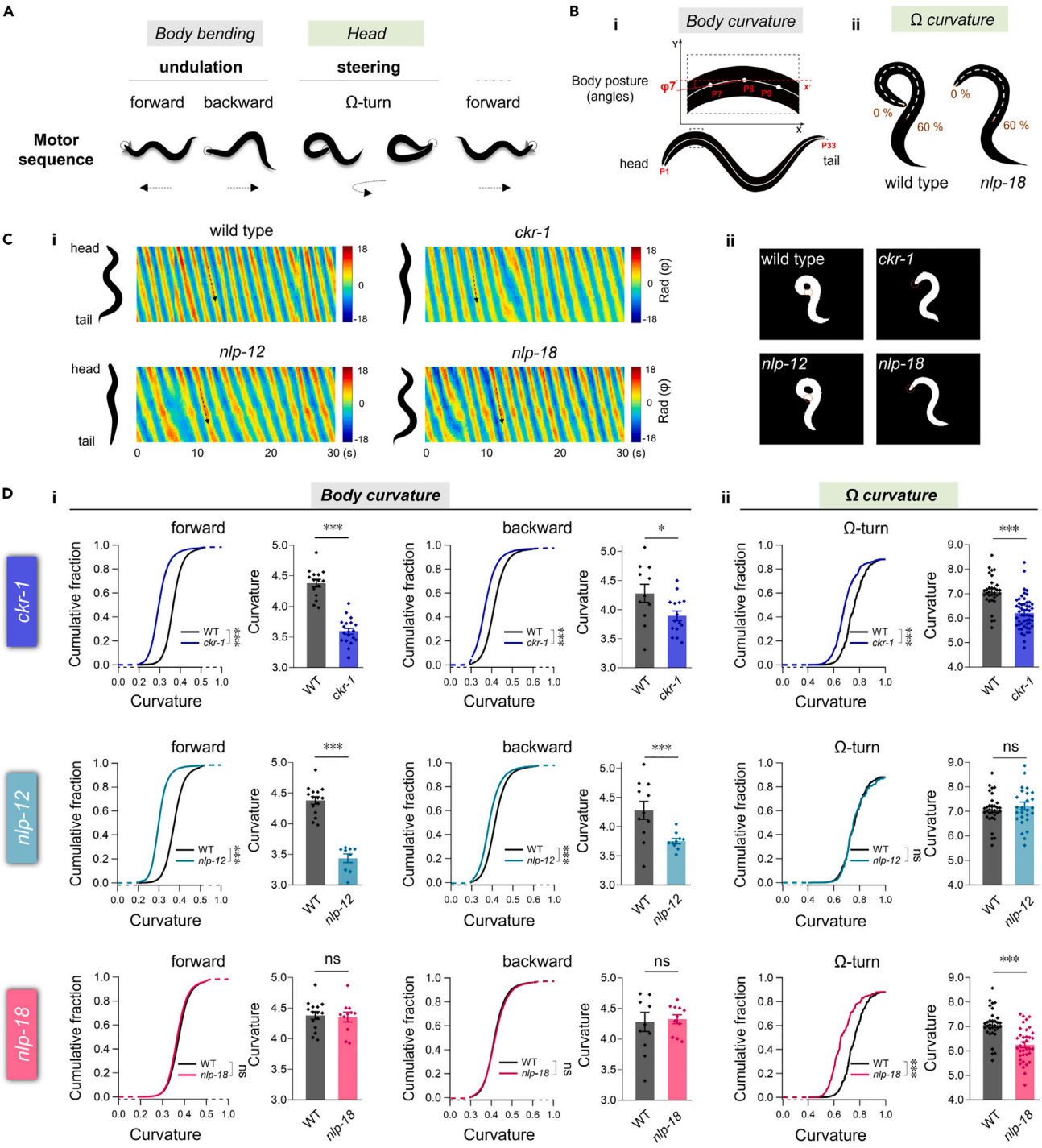

Figure 1. CKR-1 integrates the independent modulation by NLP-12 and NLP-18 for distinct motor states

(A) A schematic diagram illustrating motor sequences, including forward, backward, and Ω-turn movements. The undulation amplitude during forward and backward motions represents body bending. Head Ω-turn indicates the capacity for head steering. Black circles represent the head, and dashed arrows signify movement orientation.

(B) Schematic representation of the method used to measure body curvature (i) and head Ω curvature (ii). The body was partitioned into 32 "body segments" for curvature analysis. Body curvature and Ω curvature (0%–60% anterior part) were calculated using MATLAB.

Figure 1. *Continued*

(C) i: Representative curvature kymograms along the entire body of free-moving animals in wild type and respective mutants. ii: Representative head bending states in various genotypes.

(D) Distribution and quantification of all body curvatures of forward and backward (i) and Ω curvature (ii) in wild type, *ckr-1*, *nlp-12*, and *nlp-18* mutants ($n \geq 15$ animals). i: Every dot means one animal. ii: Every dot represents once turn. Curvature differences were analyzed using the Kolmogorov-Smirnov test. Average curvatures were plotted and analyzed using Student's *t test*. ns, no significance, *$p < 0.05$, ***$p < 0.001$. All data are expressed as mean ± SEM.

NLP-12/NLP-18's actions on body bending/head steering further supports the notion that different neuropeptides can independently modulate specific motor states through the activation of a shared receptor, CKR-1, in a context-dependent manner. Furthermore, the ability of CKR-1 to independently regulate body bending and head steering implies that a single receptor can play multiple functional roles. This highlights the complexity of neuromodulatory mechanisms in coordinating diverse motor behaviors in the nematode.

The consistent reduction in body curvature during both forward and backward movements in both *nlp-12* and *ckr-1* mutants led us to select the forward body curvature, as a unified parameter for further analyses. This allows us to focus on understanding how CKR-1 integrates and processes information from different neuropeptides to regulate distinct motor behaviors. By utilizing the body curvature as a common readout, we aim to elucidate the intricate mechanisms underlying CKR-1's ability to coordinate head steering and undulation body bending in response to the activation of NLP-12 and NLP-18.

Ectopic cross-expression of NLP-18 in DVA or NLP-12 in ASI cannot rescue body curvature or Ω curvature

Neuromodulation can exert its effects both within the synapse and in extra-synaptic regions.[24] In light of this, we investigated whether the independent modulation of NLP-12 and NLP-18 exhibits neuronal specificity. To test this, we ectopically cross-expressed NLP-12 and NLP-18 in reciprocal functional neurons.

Previous studies had implicated that NLP-12 is expressed and functional in the individual DVA neuron.[1] We then detected the expression pattern and examined the neuronal requirement of NLP-12. Consistently, when using its own promoter (P*nlp-12*::GFP), expression of *nlp-12* was observed exclusively in the single DVA neuron, with minor expression in the pharyngeal procorpus (Figure 2A). Neuronal-specific restoration of NLP-12 expression in DVA fully rescued the body curvature in *nlp-12* mutants (Figure 2B). Interestingly, removal of the *nlp-12* in the *ckr-1* mutant did not further decrease the body curvature (Figure 2B). *nlp-12; ckr-1* double mutants did not alter the Ω curvature defect of the *ckr-1* mutant (Figure 2C). These results indicate that the body bend regulation by *ckr-1* may be derived from NLP-12 peptides secreted from DVA. Importantly, when we ectopically expressed functional NLP-18 in DVA neuron, neither body curvature nor Ω curvature was rescued (Figure 2D). This result suggests that either NLP-18 is non-functional in DVA or ectopic expressed NLP-18 cannot be delivered to appropriate place.

We recently elucidated that NLP-18 primarily promotes head steering from the ASI sensory neuron.[21] When functional NLP-12 was expressed in ASI, the Ω curvature defect in the *nlp-18* mutant was not restored (Figure 2Eii). However, although the body curvature is not changed in *nlp-18* mutant, ASI expression of NLP-12 resulted in a significant increase of the body curvature (Figure 2Ei). The observation may be attributed to the characteristics of the ASI neuron, which is a multifunctional neuron containing and releasing various neuropeptides.[25–27]

In conclusion, these results collectively demonstrate that the ectopic cross-expression of NLP-18 in DVA or NLP-12 in ASI does not independently rescue body curvature or Ω curvature, indicating that NLP-12 and NLP-18 exert their physiological functions specifically within their dedicated neurons.

Motor nerve transmission is not impaired in *ckr-1*, *nlp-12*, and *nlp-18*

CKR-1 is essentially required for the modulation of two motor states; however, the neuronal basis remains unknown. The *C. elegans* motor circuit consists of A and B-type cholinergic neurons, which execute local body bending, and SMD neurons, also cholinergic, which regulate the swing of the head.[28,29] To address this question, we performed *in situ* electrophysiological recordings in the mid-frontal body region of *C. elegans* at the neuromuscular junction (NMJ), a site where both body bending and head steering may occur.

The endogenous spontaneous miniature postsynaptic currents (minis) were first recorded on the body wall muscles at a holding potential of −60 mV.[30] However, neither the frequency nor the amplitude of the minis showed any difference between *ckr-1* mutants and wild-type animals (Figures 3A and 3B). The same results were also observed in *nlp-12* and *nlp-18* mutants. Moreover, the irrelevance of CKR-1 signaling with motor nerve transmission was further verified in *nlp-12; ckr-1* and *nlp-18; ckr-1* double mutants (Figures 3A and 3B). These results indicate that the CKR-1 signaling pathway appears to be dispensable for neurotransmission at the *C. elegans* NMJ.

To further verify whether NLP-12, NLP-18, and CKR-1 influence nerve conduction, we utilized a transgenic strain expressing the optogenetic channel rhodopsin (ChR2) in excitatory cholinergic neurons (*zxIs6*), enabling reliable measurement of evoked neurotransmission in *C. elegans*.[31] Upon exposure to all-trans retinal, transient blue light (460 ± 5 nm, 3.75 mW/m^2 for 10 ms) evoked robust excitatory postsynaptic currents (EPSCs). However, both the EPSC amplitude and half-width showed no significance difference between the wild type and the aforementioned single or double mutants (Figures 3C and 3D). Thus, the evoked neurotransmission is also not impaired in *ckr-1*, *nlp-12*, and *nlp-18* mutants.

CKR-1 functions in a single head motoneuron SMD

If the excitatory A and B-type motor neurons (MNs) that make up the NMJs are not essential for CKR-1's function, the question arises: where precisely does CKR-1 operate to modulate the two motor states? To pinpoint the specific site of CKR-1's action, we investigated its expression

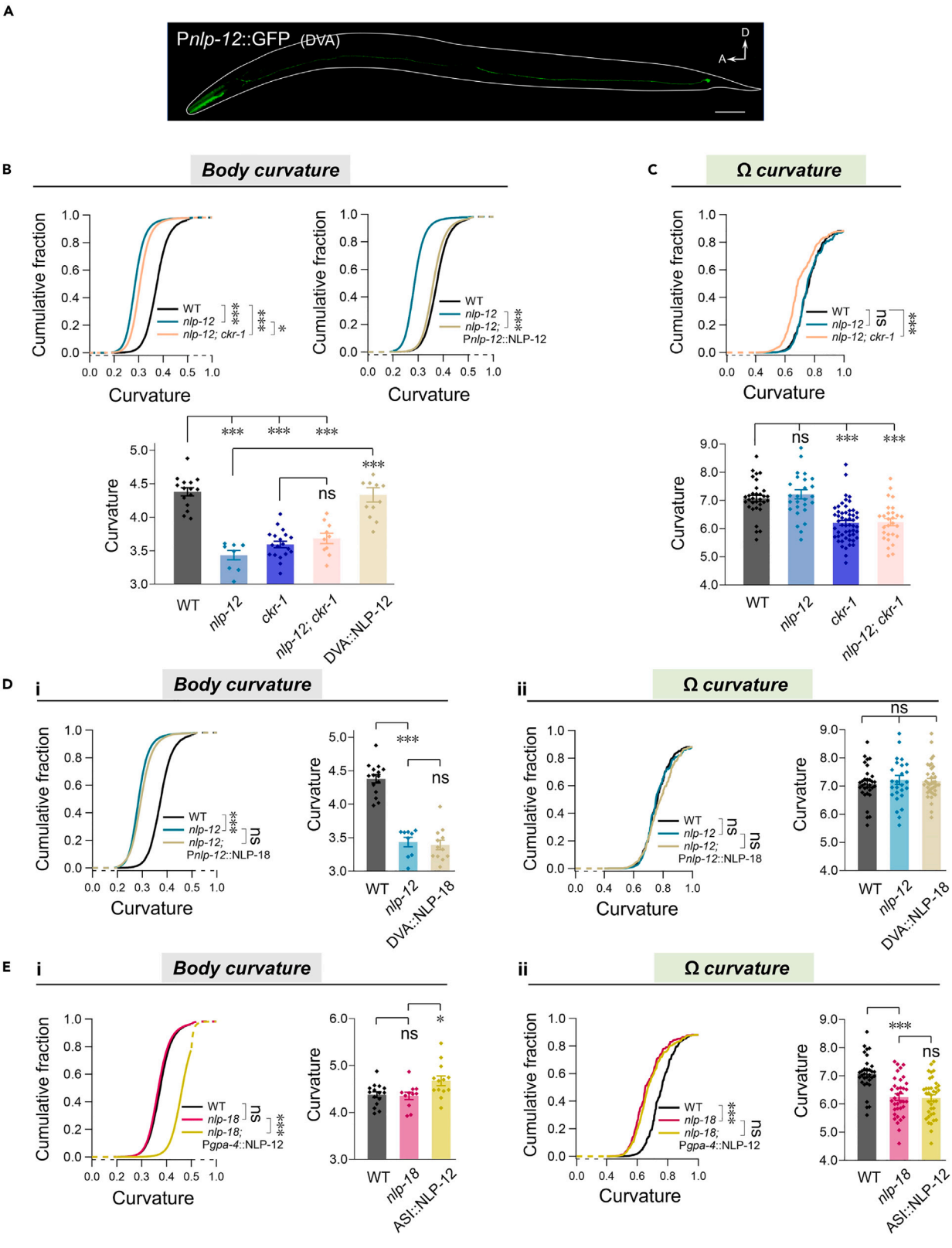
A
Pnlp-12::GFP (DVA)
D
A
B
Body curvature
Cumulative fraction
Curvature
WT
nlp-12
nlp-12; ckr-1
nlp-12;
Pnlp-12::NLP-12
DVA::NLP-12
C
Ω curvature
ns
D
i
Body curvature
Pnlp-12::NLP-18
ii
Ω curvature
E
i
Body curvature
nlp-18
nlp-18;
Pgpa-4::NLP-12
ASI::NLP-12
ii
Ω curvature

Figure 2. Cross-expression of NLP-18 and NLP-12 in DVA and ASI fails to rescue body curvature and Ω curvature

(A) Expression pattern of *nlp-12* driven by its endogenous promoter. GFP was observed in DVA neuron and pharynx procorpus. A denotes anterior, and D denotes dorsal. Scale bar, 100 μm.

(B and C) The distribution and quantification of body curvature (B) and Ω curvature (C) (n ≥ 8 animals). DVA-specific expression of NLP-12 restored reduced body curvature (B). Deletion of *nlp-12* in *ckr-1* mutants did not further decrease body or Ω curvature in *ckr-1* mutants.

(D and E) Distribution and quantification of body curvature (i) and Ω curvature (ii) by expressing NLP-18 in DVA neurons in *nlp-12* mutants and expressing NLP-12 in ASI using the P*gpa-4* promoter in *nlp-18* mutants (n ≥ 9 animals). i: Every dot means one animal. ii: Every dot represents once turn. Curvature differences were analyzed using the Kolmogorov-Smirnov test. Average curvatures were plotted and analyzed using one-way ANOVA. ns, no significance, *p < 0.05, ***p < 0.001. All data are expressed as mean ± SEM.

pattern. The transcriptional receptor for CKR-1 showed strong expression in head motor neuron SMD, interneuron AIB, along with noticeable expression in A, B, and D-MNs (Figures 4A and 4B). Consistent with the electrophysiological results, restoring CKR-1 expression in A, B, or D-MNs did not rescue the body curvature or Ω curvature (Figures S2A and S2B). As previously reported, CKR-1 primarily expresses in SMD and AIB neurons, enhancing steering signals.[21] SMD neurons also serve as functional neurons regulating head oscillation and body bending.[29,32] To assess their requirement, we restored CKR-1 expression using its endogenous promoter (P*ckr-1*) in *ckr-1* mutants, leading to full restoration of body curvature and Ω curvature to wild-type levels (Figures 4C and 4D). Similarly, expressing CKR-1 in SMD neurons (P*flp-22*) fully rescued the observed defects (Figures 4C and 4D), suggesting the sufficiency of SMD neurons in CKR-1's modulation of both motor states. Overexpression of CKR-1 in AIB interneurons (P*npr-9*) also rescued Ω curvature and partially restored body curvature.

To validate these findings without overexpression, we utilized tissue-specific depletion of CKR-1. We employed a repurposed endogenous ubiquitin system to reduce the protein level of CKR-1.[33] Briefly, we tagged the endogenous *ckr-1* locus with ZF1, an E3-recognition target signal for the ZIF-1 ligase, and received *ckr-1*:ZF1 animals (GB01). No motor differences were observed between GB01 and wild-type N2 animals (Figures S3A–S3C). However, when ZIF-1 was expressed in targeted neurons, endogenous CKR-1 proteins are degraded by ZIF-1 in a cell-specific manner (STAR Methods). Employing this non-neuronal ubiquitin system for targeted protein reduction, we observed a remarkable decrease in body curvature and Ω curvature when CKR-1 was knocked down in all CKR-1 neurons or specifically in SMD neurons (Figures 4E and 4F). This confirms the essential role of SMD neurons in CKR-1's modulation of body bending and head steering. Intriguingly, knockdown of CKR-1 in AIB interneurons reduced Ω curvature but not body curvature, indicating AIB's significance in head steering regulation. No significance changes were observed when CKR-1 was knocked down in A, B, or D-MNs neurons (Figures S2C and S2D).

In conclusion, our results collectively demonstrate that a single head motoneuron SMD is essential for CKR-1's neuromodulation in both motor states.

Different sensitivity of CKR-1 to NLP-12 and NLP-18

NLP-12 and NLP-18 independently modulate body bending and head steering through a common GPCR CKR-1 in a single neuron SMD. However, the mechanism underlying this differential regulation remains unclear. We speculate that this may be due to differences in ligand/receptor activation capacity or kinetics. To test the possibility, we first performed the *in vitro* experiment by puffing synthetic NLP-12/NLP-18 peptides to the *X. laevis* oocyte with different concentration (Figure 5A). We found that robust currents were evoked by the separate or simultaneous application of NLP-12a (1 μM) and NLP-12b (1 μM), which are two predicated mature peptides from NLP-12 precursor protein[12] (Figures S4A and S4B). This result is consistent with calcium responses in Chinese hamster ovarian cells expressing CKR-1[7], and it demonstrates that NLP-12, similar to NLP-18, acts as another ligand of CKR-1. Furthermore, both NLP-12 and NLP-18 exhibit dose-dependent activation of CKR-1. Although the peak currents evoked by saturated NLP-12 were similar to those evoked by saturated NLP-18, the EC_{50} achieved with the same concentration of NLP-12a was 26.5 nM, which is approximately twice that of NLP-18a, which had an EC_{50} of approximately 13.6 nM (Figure 5B). The activation time constant (τ) showed no difference between all individual peptides from NLP-12 and NLP-18 (Figure S4C).

These results denote that CKR-1 exhibits different sensitivity to NLP-12 and NLP-18.

Higher Ca^{2+} activity is evoked by NLP-18 in SMD *in vivo*

We then asked whether the *in vitro* results are also applicable *in vivo*. Alternatively, could NLP-12 activate endogenous CKR-1 in *C. elegans* neurons *in vivo* differently from NLP-18? To answer this question, we expressed GCaMP6s, a calcium indicator, in the key SMD neurons, and assessed the calcium dynamics evoked by synthesized NLP-12 and NLP-18 in dissected *C. elegans* preparation, respectively (Figure 5C). NLP-12 peptides (mixed NLP-12a and NLP-12b, 1 μM each) evoked substantial Ca^{2+} transients in SMD neurons (Figure 5C). Moreover, the Ca^{2+} response was abolished in *ckr-1* mutants and restored by CKR-1 expression in SMD neurons, suggesting that SMD could be activated by NLP-12 that depending on the activation of CKR-1. Importantly, compared to the Ca^{2+} transients evoked by NLP-18, the peak amplitude evoked by NLP-12 was smaller (Figure 5D). The activation dynamics (10%–90% raise time) is a little bit faster compared to those of NLP-18 (Figure 5E). This result denotes that, as the ligand for CKR-1, NLP-18 displays a higher activation capacity of CKR-1.

In summary, our research sheds light on how the CKR-1 receptor orchestrates two distinct motor states within a single head motoneuron. This regulation is mediated by two independent neuropeptides, NLP-12 and NLP-18, which exhibit different activation characteristics and are secreted from different sensory neurons.

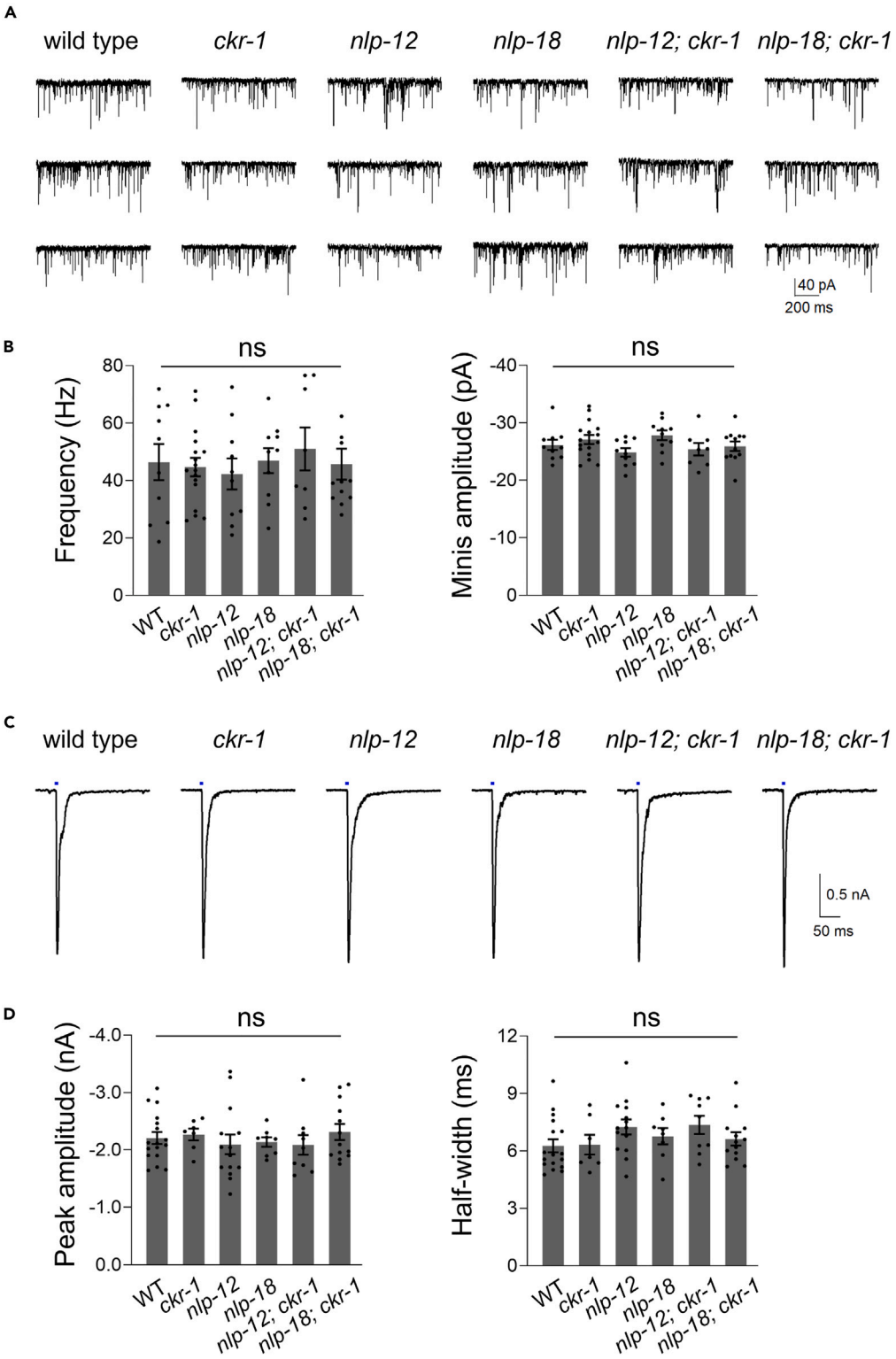

Figure 3. CKR-1 signaling does not impact neurotransmission at the NMJ

(A) Representative traces of spontaneously released miniature post-synaptic currents (minis) in different genotypes. Minis were recorded at the NMJ preparation while holding the body wall muscle cells at −60 mV.

Figure 3. *Continued*

(B) Quantification of the minis frequency and minis amplitude (n ≥ 8 animals).

(C) Representative traces of evoked post-synaptic currents through the activation of cholinergic motor neurons with blue light (460 ± 5 nm, 3.75 mW/m^2 for 10 ms). The blue line indicates the onset of blue light.

(D) Quantification of the amplitude and half-width of evoked currents (n ≥ 7 animals). Every dot means one animal. Average currents were plotted and analyzed using one-way ANOVA. ns, no significance. All data are expressed as mean ± SEM.

DISCUSSION

Neuropeptidergic systems play pivotal roles in modulating neuronal function, thereby shaping diverse behavioral responses. However, our understanding of how a single neuromodulation receptor perceives multiple modulators to coordinate distinct behaviors remains limited. In this study, we investigated the role of the neuropeptide receptor CKR-1 in modulating two motor states, undulation body bending and head steering in the nematode *C. elegans*. Our findings revealed that CKR-1 is crucially involved in regulating both motor states, and its function is independent of a shared mechanistic pathway. Notably, two distinct neuropeptides, NLP-12 and NLP-18, independently regulate body bending and head steering, respectively, by activating CKR-1. Through *in vitro* experiments, we demonstrated that CKR-1 exhibits differential sensitivities to NLP-12 and NLP-18, with NLP-18 displaying higher potency. Moreover, *in vivo* experiments unveiled that NLP-18 induces greater Ca^{2+} activity in SMD neurons compared to NLP-12. Furthermore, CKR-1's regulatory role does not interfere with motor nerve transmission at the neuromuscular junction. Overall, our findings provide valuable insights into the complex neuromodulatory mechanism by which CKR-1, in conjunction with different neuropeptides, coordinates distinct motor states in *C. elegans*.

Our study showed compelling evidence that the neuropeptide receptor CKR-1 in *C. elegans* plays a remarkable role in sensing and integrating multiple neuropeptides to coordinate distinct motor behaviors. It provides a good paradigm for studying how a GPCR receptor perceives different neuropeptides for regulating different behaviors. Specifically, we identified two distinct neuropeptides, NLP-12 and NLP-18, which independently regulate undulation body bending and escape head steering, respectively, by activating CKR-1. This receptor multitasking phenomenon challenges the conventional notion that neuropeptides typically activate specific receptors to regulate distinct behaviors. Instead, our findings suggest that CKR-1 has the unique capacity to respond to and integrate signals from different neuropeptides, thereby enabling the fine-tuned control of diverse motor states.

This ability of CKR-1 to perceive multiple modulators suggests that neuropeptides may play a broader role in neural circuits than previously thought. Regulation of multiple functions by a single neuropeptide receptor is not uncommon, for example, the neuropeptide F receptor (sNPFR) influences many physiological processes, including feeding, growth, and olfactory memory,[34,35] neuropeptide FF receptors 1 and 2 regulate memory, autonomic regulation, neuroendocrine regulation, and adipocyte metabolism in rats,[36,37] and neuropeptide Y receptors mediate multiple essential physiological processes, such as food intake, vasoconstriction, sedation, and memory retention in humans.[38–40] However, such fine-tuning of diverse motor states by a neuropeptide receptor in a single neuron is surprising, and the process of how this is achieved is intriguing. The complexity and specificity of neuropeptide signaling in neural circuits are essential for maintaining proper physiological functions. Neuropeptides act as messengers, transmitting information between neurons and target cells within specific regions of the nervous system. In addition to the selective expression of receptors, differences in receptor sensitivity to ligands also play an important role in achieving specificity in neuropeptide signaling.

Our study also sheds light on the potential mechanism underlying the signaling integration by CKR-1 to coordinate distinct motor states within a single motoneuron, SMD, which possibly includes: (1) Functional neuropeptide secretion: Functional neuropeptides are secreted from different sensory neurons, for example, NLP-12 from proprioceptive neuron DVA and NLP-18 from polymodal sensory neuron ASI, respectively. Different sensory neurons perceive different stimulus patterns, like DVA is a mechanosensitive neuron that senses muscular mechanical stimulus,[8,41] and ASI is a polymodal neuron and receives multiplex stimuli.[26] Therefore, the secretion of NLP-12 and NLP-18 may depend on the stimulus type, which associates with different behavioral regulation. (2) Synaptic-binding sites: DVA and ASI both send direct chemical synapses to and establish hard-wiring connection with SMD neurons.[42–44] The synaptic sites, however, are not exactly the same. SMD neurons may use different synaptic-binding sites to enhance or coordinate two motor states, although the extrasynaptic neuropeptidergic signaling is probably involved as well. (3) Differential sensitivity and kinetics: The differential sensitivities of CKR-1 to NLP-12 and NLP-18, with NLP-18 displaying higher potency, indicate that this receptor can discern the strengths of different neuropeptide signals. *In vivo* calcium imaging experiments also revealed that NLP-18 induces higher Ca^{2+} activity in SMD neurons compared to NLP-12. Beside, NLP-12 had a faster activation of CKR-1 in SMD than did NLP-18, although *in vitro* recombinant currents in oocytes did not reveal significant differences. Thus, the CKR-1 activation kinetics by the two neuropeptides is also not identical. These findings suggest that CKR-1 modulates motor behaviors in a single motoneuron by finely tuning its responses to varying neuropeptide inputs with different sensitivity/kinetics, synaptic activation sites, and/or type of stimulation.

Furthermore, our electrophysiological experiments demonstrated that NLP-12, NLP-18, and CKR-1 do not directly regulate motor neuron activity, indicating that CKR-1-modulated SMD neurons likely act as a central integrator of neuropeptide signals rather than solely controlling A, B, and D-MNs excitability. This integration mechanism in SMD likely involves complex intracellular signaling pathways but could also be implied by its features of the neuronal wiring and intracellular calcium activity, like oscillated and CPG-like rhythmic activity during both body and body bending.[45,46]

The fine-tuned regulation of distinct motor states by CKR-1 and different neuropeptides may hold significant implications for understanding the adaptability and plasticity of neural circuits underlying motor behaviors. By independently modulating body bending and head

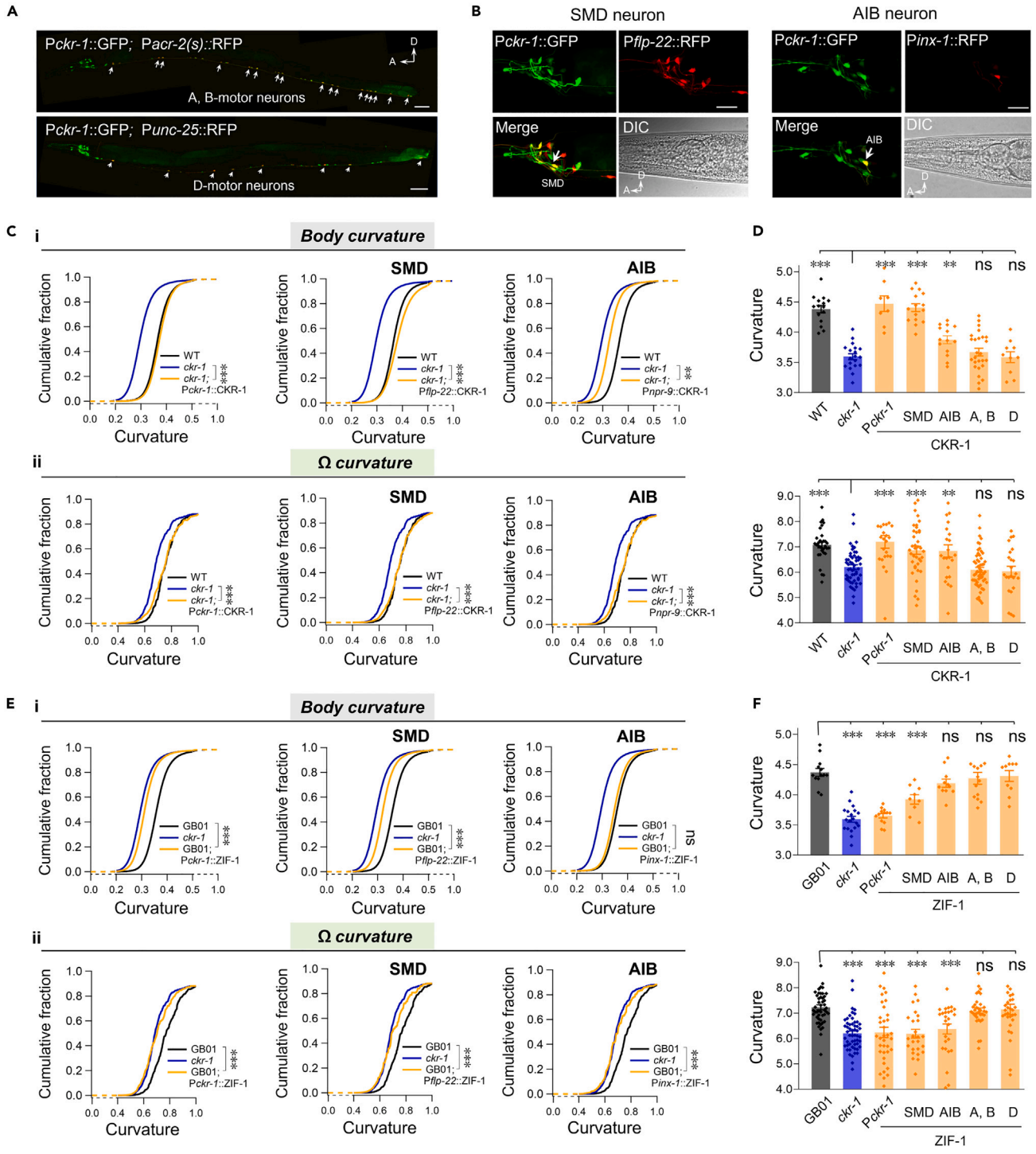

Figure 4. CKR-1 governs two distinct motor states through a singular SMD motoneuron

(A) Co-localization of *ckr-1* in A-, B-, and D-motor neurons. P*ckr-1*::GFP was found to co-localize with P*acr-2(s)*-driven RFP in cholinergic A, B-motor neurons and with P*unc-25*-driven RFP in GABAergic D-motor neurons. Scale bar, 100 μm.

(B) Co-localization of *ckr-1* in SMD and AIB neurons. SMD neuron was marked by P*flp-22*:: RFP, while AIB neuron was labeled by P*inx-1*::RFP. A denotes anterior, and D denotes dorsal. Scale bar, 20 μm.

(C) Distribution of body curvature (i) and Ω curvature (ii). Body curvature and Ω curvature defects in *ckr-1* mutant were fully restored by CKR-1 expression in SMD neurons and partially restored in AIB interneurons.

Figure 4. *Continued*

(D) Quantification of average body curvature (top) and Ω curvature (bottom) (n ≥ 15 animals). Every dot means one animal.

(E) Distribution of body curvature (i) and Ω curvature (ii) in GB01, *ckr-1* mutant and transgenic lines with SMD and AIB-specific expression of ZIF-1 in GB01 background, respectively. Body curvature was reduced by ZIF-1 expression in SMD but not in AIB, while both body and Ω curvatures were reduced by ZIF-1 expression in SMD neurons.

(F) Quantification of body curvature (top) and Ω curvature (bottom) (n ≥ 15 animals). Every dot represents once turn. Kolmogorov-Smirnov test was used to analyze the distribution differences of body curvature and Ω curvature, ns, not significant, **p < 0.01, ***p < 0.001. Average curvatures were plotted and analyzed using one-way ANOVA. ns, no significance **p < 0.01, ***p < 0.001. All data are expressed as mean ± SEM.

steering, NLP-12 and NLP-18 contribute to the precise control of directional locomotion and escape responses, respectively. This level of specificity allows animals to effectively respond to varying environmental cues and internal states, such as food abundance and hunger status.[7] Understanding the regulatory mechanisms of CKR-1 and neuropeptides in coordinating motor states not only advances our knowledge of *C. elegans* neurobiology but also holds implications for unraveling neuromodulatory processes in more complex organisms, including mammals.

In conclusion, our study demonstrates that CKR-1, as a CCK receptor in *C. elegans*, integrates signals from multiple neuropeptides, NLP-12 and NLP-18, to orchestrate distinct motor behaviors. Our findings pave the way for future investigations into the intracellular signaling cascades and molecular mechanisms underlying the multitasking ability of CKR-1. The complexity of neuromodulation revealed by our study may yield insights into the pathogenesis of motor disorders in humans.

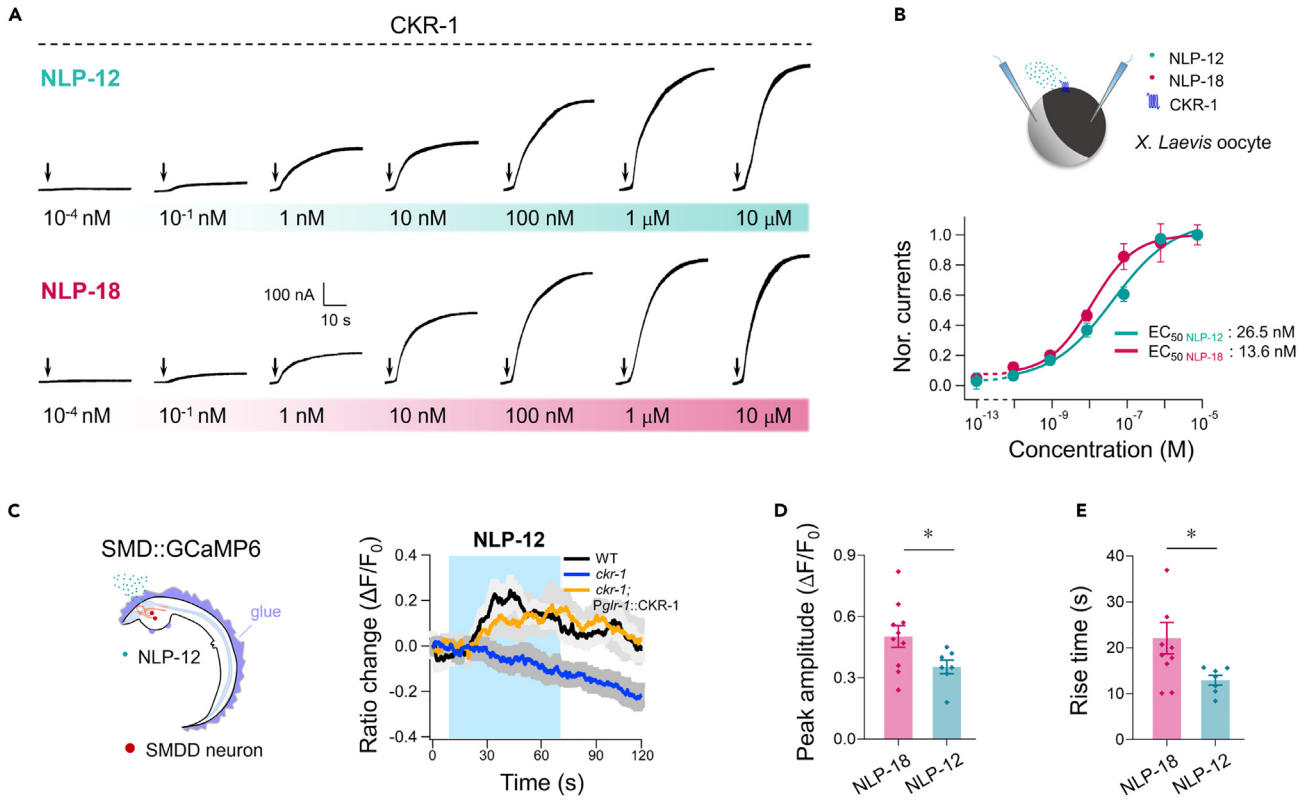

Figure 5. NLP-12 activates CKR-1 directly, but with lower sensitivity compared to NLP-18

(A) Representative current traces evoked by synthetic NLP-12a and NLP-18a peptides at different concentration in *X. laevis oocyte*. Arrows indicate the onset of peptide puffing.

(B) Schematic diagram depicting the expression of CKR-1 in oocyte (*Top*). Dose-response curve of NLP-12a and NLP-18a-evoked currents, revealing an EC_{50} of NLP-12 (26.5 nM) compared to NLP-18 (13.6 nM), fitted by the Hill equation (*Bottom*).

(C) *Left*, schematic diagram of dissected preparation with neuropeptides puffing onto SMD. *Right*, NLP-12 neuropeptides (mixed NLP-12a/b, 1 μM each) evoked robust Ca^{2+} transient in SMD neurons. NLP-12-evoked Ca^{2+} transients were terminated in the *ckr-1* mutant (*blue line*), but rescued by expression of CKR-1 in SMD neurons (*orange line*).

(D and E) Comparison of the differences in Ca^{2+} peak amplitude and rise-time evoked by NLP-12 and NLP-18 peptides (n ≥ 7 animals). Every dot means one animal. These data were plotted and analyzed using Student's *t test*. All data are expressed as mean ± SEM. *p < 0.05.

Limitations of the study

In this study, we have shown that a neuropeptide receptor, CKR-1, integrates two motor states via two neuropeptides: NLP-18 secreted from ASI neurons and NLP-12 from DVA neurons. Interestingly, these two motor states operate on different time scales, leading to an essential question about the mechanisms of spatiotemporal physiological processes. In other words, the specific activation modes or spatial specificity of these processes remain unclear. Moreover, whether the release of neuropeptides by different neurons is persistent or state dependent is yet to be determined. These are the key areas that warrant further investigation.

STAR★METHODS

Detailed methods are provided in the online version of this paper and include the following:

- KEY RESOURCES TABLE
- RESOURCE AVAILABILITY
  - Lead contact
  - Materials availability
  - Data and code availability
- EXPERIMENTAL MODEL AND STUDY PARTICIPANT DETAILS
  - Worm maintenance and strains
- METHOD DETAILS
  - Molecular biology
  - Behavioral analyses
  - *In situ* electrophysiology and calcium imaging
  - Confocal fluorescence microscopy
  - ZIF-1-ZF1 system
  - Oocytes expression and two electrode voltage-clamp
- QUANTIFICATION AND STATISTICAL ANALYSIS

SUPPLEMENTAL INFORMATION

Supplemental information can be found online at https://doi.org/10.1016/j.isci.2024.109390.

ACKNOWLEDGMENTS

We thank Mei Zhen for insightful discussion and valuable experimental suggestions. This research was supported by the National Natural Science Foundation of China (32300984), the Major International (Regional) Joint Research Project (32020103007), the National Key Research and Development Program of China (2022YFA1206001), the National Natural Science Foundation of China (32371189 and 31871069), the Young Scientists Fund of the National Natural Science Foundation of China (32300834), the Overseas High-level Talents Introduction Program. We thank *Caenorhabditis Genetics Center*, which is funded by the NIH Office of Research Infrastructure Programs (P40 OD010440), for strains.

AUTHOR CONTRIBUTIONS

S.G. conceived experiments. L.C., P.S., Y.W., and Y.L. performed experiments and analyzed data. L.-M.C. contributed experiments. S.G. and L.C. wrote the manuscript.

DECLARATION OF INTERESTS

The authors declare no conflict of interest.

Received: September 27, 2023
Revised: December 22, 2023
Accepted: February 28, 2024
Published: March 2, 2024

REFERENCES

1. Bhattacharya, R., Touroutine, D., Barbagallo, B., Climer, J., Lambert, C.M., Clark, C.M., Alkema, M.J., and Francis, M.M. (2014). A conserved dopamine-cholecystokinin signaling pathway shapes context-dependent *Caenorhabditis elegans* behavior. PLoS Genet. *10*, e1004584. https://doi.org/10.1371/journal.pgen.1004584.
2. Grillner, S., and Jessell, T.M. (2009). Measured motion: searching for simplicity in spinal locomotor networks. Curr. Opin. Neurobiol. *19*, 572–586. https://doi.org/10.1016/j.conb.2009.10.011.
3. Marder, E., O'Leary, T., and Shruti, S. (2014). Neuromodulation of circuits with variable parameters: single neurons and small circuits reveal principles of

state-dependent and robust neuromodulation. Annu. Rev. Neurosci. *37*, 329–346. https://doi.org/10.1146/annurev-neuro-071013-013958.

4. Kim, S.M., Su, C.Y., and Wang, J.W. (2017). Neuromodulation of Innate Behaviors in *Drosophila*. Annu. Rev. Neurosci. *40*, 327–348. https://doi.org/10.1146/annurev-neuro-072116-031558.
5. Speranza, L., di Porzio, U., Viggiano, D., de Donato, A., and Volpicelli, F. (2021). Dopamine: The Neuromodulator of Long-Term Synaptic Plasticity, Reward and Movement Control. Cells *10*. https://doi.org/10.3390/cells10040735.
6. Shine, J.M. (2023). Neuromodulatory control of complex adaptive dynamics in the brain. Interface Focus *13*, 20220079. https://doi.org/10.1098/rsfs.2022.0079.
7. Ramachandran, S., Banerjee, N., Bhattacharya, R., Lemons, M.L., Florman, J., Lambert, C.M., Touroutine, D., Alexander, K., Schoofs, L., Alkema, M.J., et al. (2021). A conserved neuropeptide system links head and body motor circuits to enable adaptive behavior. Elife *10*, e71747. https://doi.org/10.7554/eLife.71747.
8. Hu, Z., Pym, E.C.G., Babu, K., Vashlishan Murray, A.B., and Kaplan, J.M. (2011). A neuropeptide-mediated stretch response links muscle contraction to changes in neurotransmitter release. Neuron *71*, 92–102. https://doi.org/10.1016/j.neuron.2011.04.021.
9. Cohen, M., Reale, V., Olofsson, B., Knights, A., Evans, P., and de Bono, M. (2009). Coordinated regulation of foraging and metabolism in *C. elegans* by RFamide neuropeptide signaling. Cell Metab *9*, 375–385. https://doi.org/10.1016/j.cmet.2009.02.003.
10. Deffains, M., and Bergman, H. (2015). Striatal cholinergic interneurons and cortico-striatal synaptic plasticity in health and disease. Mov. Disord. *30*, 1014–1025. https://doi.org/10.1002/mds.26300.
11. Avila, A., Cardona, X., Bello, J., Maho, P., Sastre, F., and Martin-Baranera, M. (2011). Impulse control disorders and punding in Parkinson's disease: the need for a structured interview. Neurologia *26*, 166–172. https://doi.org/10.1016/j.nrl.2010.09.007.
12. Li, C., and Kim, K. (2008). Neuropeptides (WormBook), pp. 1–36. https://doi.org/10.1895/wormbook.1.142.1.
13. Frooninckx, L., Van Rompay, L., Temmerman, L., Van Sinay, E., Beets, I., Janssen, T., Husson, S.J., and Schoofs, L. (2012). Neuropeptide GPCRs in *C. elegans*. Front. Endocrinol. *3*, 167. https://doi.org/10.3389/fendo.2012.00167.
14. Bhat, U.S., Shahi, N., Surendran, S., and Babu, K. (2021). Neuropeptides and Behaviors: How Small Peptides Regulate Nervous System Function and Behavioral Outputs. Front. Mol. Neurosci. *14*, 786471. https://doi.org/10.3389/fnmol.2021.786471.
15. Nassel, D.R., and Winther, A.M. (2010). *Drosophila* neuropeptides in regulation of physiology and behavior. Prog Neurobiol *92*, 42–104. https://doi.org/10.1016/j.pneurobio.2010.04.010.
16. Hökfelt, T., Broberger, C., Xu, Z.Q., Sergeyev, V., Ubink, R., and Diez, M. (2000). Neuropeptides–an overview. Neuropharmacology *39*, 1337–1356. https://doi.org/10.1016/s0028-3908(00)00010-1.
17. Janssen, T., Lindemans, M., Meelkop, E., Temmerman, L., and Schoofs, L. (2010). Coevolution of neuropeptidergic signaling systems: from worm to man. Ann. N. Y. Acad. Sci. *1200*, 1–14. https://doi.org/10.1111/j.1749-6632.2010.05506.x.
18. Russo, A.F. (2017). Overview of Neuropeptides: Awakening the Senses? Headache *57* (*Suppl 2*), 37–46. https://doi.org/10.1111/head.13084.
19. Ringstad, N., and Horvitz, H.R. (2008). FMRFamide neuropeptides and acetylcholine synergistically inhibit egg-laying by *C. elegans*. Nat. Neurosci. *11*, 1168–1176. https://doi.org/10.1038/nn.2186.
20. Cockx, B., Van Bael, S., Boelen, R., Vandewyer, E., Yang, H., Le, T.A., Dalzell, J.J., Beets, I., Ludwig, C., Lee, J., and Temmerman, L. (2023). Mass Spectrometry-Driven Discovery of Neuropeptides Mediating Nictation Behavior of Nematodes. Mol. Cell. Proteomics *22*, 100479. https://doi.org/10.1016/j.mcpro.2022.100479.
21. Chen, L., Liu, Y., Su, P., Hung, W., Li, H., Wang, Y., Yue, Z., Ge, M.H., Wu, Z.X., Zhang, Y., et al. (2022). Escape steering by cholecystokinin peptidergic signaling. Cell Rep. *38*, 110330. https://doi.org/10.1016/j.celrep.2022.110330.
22. Hu, Z., Vashlishan-Murray, A.B., and Kaplan, J.M. (2015). NLP-12 engages different UNC-13 proteins to potentiate tonic and evoked release. J. Neurosci. *35*, 1038–1042. https://doi.org/10.1523/JNEUROSCI.2825-14.2015.
23. Janssen, T., Meelkop, E., Lindemans, M., Verstraelen, K., Husson, S.J., Temmerman, L., Nachman, R.J., and Schoofs, L. (2008). Discovery of a cholecystokinin-gastrin-like signaling system in nematodes. Endocrinology *149*, 2826–2839. https://doi.org/10.1210/en.2007-1772.
24. Nadim, F., and Bucher, D. (2014). Neuromodulation of neurons and synapses. Curr. Opin. Neurobiol. *29*, 48–56. https://doi.org/10.1016/j.conb.2014.05.003.
25. Bargmann, C.I., and Horvitz, H.R. (1991). Control of larval development by chemosensory neurons in *Caenorhabditis elegans*. Science *251*, 1243–1246. https://doi.org/10.1126/science.2006412.
26. Pandey, P., Bhat, U.S., Singh, A., Joy, A., Birari, V., Kadam, N.Y., and Babu, K. (2021). Dauer Formation in *C. elegans* Is Modulated through AWC and ASI-Dependent Chemosensation. eNeuro *8*. https://doi.org/10.1523/ENEURO.0473-20.2021.
27. You, Y.J., Kim, J., Raizen, D.M., and Avery, L. (2008). Insulin, cGMP, and TGF-beta signals regulate food intake and quiescence in *C. elegans*: a model for satiety. Cell Metab *7*, 249–257. https://doi.org/10.1016/j.cmet.2008.01.005.
28. Zhen, M., and Samuel, A.D.T. (2015). *C. elegans* locomotion: small circuits, complex functions. Curr. Opin. Neurobiol. *33*, 117–126. https://doi.org/10.1016/j.conb.2015.03.009.
29. Shen, Y., Wen, Q., Liu, H., Zhong, C., Qin, Y., Harris, G., Kawano, T., Wu, M., Xu, T., Samuel, A.D., and Zhang, Y. (2016). An extrasynaptic GABAergic signal modulates a pattern of forward movement in *Caenorhabditis elegans*. Elife *5*, e14197. https://doi.org/10.7554/eLife.14197.
30. Richmond, J.E., and Jorgensen, E.M. (1999). One GABA and two acetylcholine receptors function at the *C. elegans* neuromuscular junction. Nat. Neurosci. *2*, 791–797. https://doi.org/10.1038/12160.
31. Liewald, J.F., Brauner, M., Stephens, G.J., Bouhours, M., Schultheis, C., Zhen, M., and Gottschalk, A. (2008). Optogenetic analysis of synaptic function. Nat. Methods *5*, 895–902. https://doi.org/10.1038/nmeth.1252.
32. Gray, J.M., Hill, J.J., and Bargmann, C.I. (2005). A circuit for navigation in *Caenorhabditis elegans*. Proc Natl Acad Sci USA *102*, 3184–3191. https://doi.org/10.1073/pnas.0409009101.
33. Armenti, S.T., Lohmer, L.L., Sherwood, D.R., and Nance, J. (2014). Repurposing an endogenous degradation system for rapid and targeted depletion of *C. elegans* proteins. Development *141*, 4640–4647. https://doi.org/10.1242/dev.115048.
34. Li, H., Huang, X., Yang, Y., Chen, X., Yang, Y., Wang, J., and Jiang, H. (2022). The short neuropeptide F receptor regulates olfaction-mediated foraging behavior in the oriental fruit fly Bactrocera dorsalis (Hendel). Insect Biochem. Mol. Biol. *140*, 103697. https://doi.org/10.1016/j.ibmb.2021.103697.
35. Cui, H.-y., and Zhao, Z.-w. (2020). Structure and function of neuropeptide F in insects. J. Integr. Agric. *19*, 1429–1438. https://doi.org/10.1016/s2095-3119(19)62804-2.
36. Panula, P., Aarnisalo, A.A., and Wasowicz, K. (1996). Neuropeptide FF, a mammalian neuropeptide with multiple functions. Prog. Neurobiol. *48*, 461–487. https://doi.org/10.1016/0301-0082(96)00001-9.
37. Lefrere, I., De Coppet, P., Camelin, J.C., Le Lay, S., Mercier, N., Elshourbagy, N., Bril, A., Berrebi-Bertrand, I., Feve, B., and Krief, S. (2002). Neuropeptide AF and FF modulation of adipocyte metabolism. Primary insights from functional genomics and effects on beta-adrenergic responsiveness. J. Biol. Chem. *277*, 39169–39178. https://doi.org/10.1074/jbc.M205084200.
38. Tang, T., Tan, Q., Han, S., Diemar, A., Lobner, K., Wang, H., Schuss, C., Behr, V., Morl, K., Wang, M., et al. (2022). Receptor-specific recognition of NPY peptides revealed by structures of NPY receptors. Sci. Adv. *8*, eabm1232. https://doi.org/10.1126/sciadv.abm1232.
39. Yang, Z., Han, S., Keller, M., Kaiser, A., Bender, B.J., Bosse, M., Burkert, K., Kogler, L.M., Wifling, D., Bernhardt, G., et al. (2018). Structural basis of ligand binding modes at the neuropeptide Y Y(1) receptor. Nature *556*, 520–524. https://doi.org/10.1038/s41586-018-0046-x.
40. Morales-Medina, J.C., Dumont, Y., and Quirion, R. (2010). A possible role of neuropeptide Y in depression and stress. Brain Res. *1314*, 194–205. https://doi.org/10.1016/j.brainres.2009.09.077.
41. Li, W., Feng, Z., Sternberg, P.W., and Xu, X.Z. (2006). A *C. elegans* stretch receptor neuron revealed by a mechanosensitive TRP channel homologue. Nature *440*, 684–687. https://doi.org/10.1038/nature04538.
42. Cook, S.J., Jarrell, T.A., Brittin, C.A., Wang, Y., Bloniarz, A.E., Yakovlev, M.A., Nguyen, K.C.Q., Tang, L.T., Bayer, E.A., Duerr, J.S., et al. (2019). Whole-animal connectomes of both *Caenorhabditis elegans* sexes. Nature *571*, 63–71. https://doi.org/10.1038/s41586-019-1352-7.
43. Witvliet, D., Mulcahy, B., Mitchell, J.K., Meirovitch, Y., Berger, D.R., Wu, Y., Liu, Y., Koh, W.X., Parvathala, R., Holmyard, D., et al. (2021). Connectomes across development reveal principles of brain maturation. Nature *596*, 257–261. https://doi.org/10.1038/s41586-021-03778-8.

44. White, J.G., Southgate, E., Thomson, J.N., and Brenner, S. (1986). The structure of the nervous system of the nematode *Caenorhabditis elegans*. Philos. Trans. R. Soc. Lond. B Biol. Sci. *314*, 1–340. https://doi.org/10.1098/rstb.1986.0056.

45. Gao, S., Guan, S.A., Fouad, A.D., Meng, J., Kawano, T., Huang, Y.C., Li, Y., Alcaire, S., Hung, W., Lu, Y., et al. (2018). Excitatory motor neurons are local oscillators for backward locomotion. Elife *7*. https://doi.org/10.7554/eLife.29915.

46. Fouad, A.D., Teng, S., Mark, J.R., Liu, A., Alvarez-Illera, P., Ji, H., Du, A., Bhirgoo, P.D., Cornblath, E., Guan, S.A., and Fang-Yen, C. (2018). Distributed rhythm generators underlie *Caenorhabditis elegans* forward locomotion. Elife *7*. https://doi.org/10.7554/eLife.29913.

47. Lockery, S.R., and Goodman, M.B. (2009). The quest for action potentials in *C. elegans* neurons hits a plateau. Nat. Neurosci. *12*, 377–378. https://doi.org/10.1038/nn0409-377.

48. Gao, S., and Zhen, M. (2011). Action potentials drive body wall muscle contractions in *Caenorhabditis elegans*. Proc. Natl. Acad. Sci. USA *108*, 2557–2562. https://doi.org/10.1073/pnas.1012346108.

49. Rogers, C., Reale, V., Kim, K., Chatwin, H., Li, C., Evans, P., and de Bono, M. (2003). Inhibition of *Caenorhabditis elegans* social feeding by FMRFamide-related peptide activation of NPR-1. Nat. Neurosci. *6*, 1178–1185. https://doi.org/10.1038/nn1140.

50. Oron, Y., Dascal, N., Nadler, E., and Lupu, M. (1985). Inositol 1,4,5-trisphosphate mimics muscarinic response in *Xenopus oocytes*. Nature *313*, 141–143. https://doi.org/10.1038/313141a0.

STAR★METHODS

KEY RESOURCES TABLE

REAGENT or RESOURCE	SOURCE	IDENTIFIER
Bacterial and virus strains		
OP50	CGC	http://www.cgc.edu/strain/OP50
Chemicals, peptides, and recombinant proteins		
NLP-18a	Guoping Pharmaceutical Company	ARYGFA-NH2
NLP-18b	Guoping Pharmaceutical Company	SPYRAFAFA-NH2
NLP-18c	Guoping Pharmaceutical Company	SPYRTFAFA-NH2
NLP-18d	Guoping Pharmaceutical Company	SDEENLDFLE-NH2
NLP-18e	Guoping Pharmaceutical Company	ASPYGFAFA-NH2
NLP-12a	Guoping Pharmaceutical Company	DYRPLQF-NH2
NLP-12b	Guoping Pharmaceutical Company	DGYRPLQF-NH2
ClonExpress®II One Step Cloning Kit	Vazyme Biotech co., ltd	Vazyme#C112
2 × Phanta® Max Master Mix (Dye Plus)	Vazyme Biotech co., ltd	Vazyme#P525
Gateway™ LR Clonase™ Plus Enzyme Mix	Invitrogen, Thermo Fisher Scientific	Cat#12538-013
BP Clonase™ II Enzyme Mix	Invitrogen, Thermo Fisher Scientific	Cat#11789-013
Experimental models: Organisms/strains		
N2 Bristol	This paper	Wild type
nlp-18(ok1557) II	This paper	RB1372
ckr-1(ok2502) I	This paper	RB1923
nlp-12(ok335) I	This paper	RB607
nlp-12(ok335); ckr-1(ok2502)	This paper	SGA544
nlp-12(ok335); gaaEx1182 [Pnlp-12::nlp-12::sl2dGFP; lin-44::gfp]	This paper	SGA724
nlp-12(ok335); gaaEx1224[Pnlp-12::nlp-18::sl2dGFP]	This paper	SGA816
nlp-18(ok1557); gaaEx1223[Pgpa-4::nlp-12::sl2dGFP]	This paper	SGA815
ckr-1(ok2502); gaaEx035[Pckr-1::ckr-1::s12dGFP; lin-44::gfp::3UTR	This paper	SGA35
ckr-1(ok2502); gaaEx039[Pflp-22::ckr-1::s12dGFP; lin-44::gfp]	This paper	SGA59
ckr-1(ok2502); gaaEx040[Punc-47::ckr-1::s12dGFP; lin-44::gfp]	This paper	SGA40
ckr-1(ok2502); gaaEx041[Pacr-2(s)::ckr-1::s12dGFP; lin-44::gfp]	This paper	SGA41
ckr-1(ok2502); gaaEx057[Pnpr-9::ckr-1::sl2dGFP; lin-44::gfp]	This paper	SGA57
gaaIs1; gaaEx0134[Pckr-1::ZIF-1::sl2dGFP]	This paper	SGA312
gaaIs1; gaaEx0131[Pinx-1::ZIF-1::sl2dGFP]	This paper	SGA309
gaaIs1; gaaEX0135[Pflp-22::ZIF-1::wCherry]	This paper	SGA313
gaaIs1[Pckr-1-ZF1-SL2-NLS-GFP]	This paper	GB01
gaaIs8[Pglr-1::GCaMP6.0(s)::wCherry; lin-44::gfp]	This paper	SGA284
ckr-1(ok2502); gaaIs8[Pglr-1::GCaMP6.0(s)::wCherry; lin-44::gfp]	This paper	SGA286
ckr-1; gaaIs8; gaaEx1141[Pglr-1::ckr-1::3′UTR-Pceh-63::gfp]	This paper	SGA637

(*Continued on next page*)

Continued

REAGENT or RESOURCE	SOURCE	IDENTIFIER
Recombinant DNA		
pDONR221	This paper	SG2
PDESTR4-R3II	This paper	SG4
Plin-44::GFP	This paper	SG5
Pnlp-12::nlp-12::sl2dGFP	This paper	SG618
Pnlp-12::nlp-18::sl2dGFP	This paper	SG619
Pgpa-4::nlp-12::sl2dGFP	This paper	SG620
Pnlp-12::GFP	This paper	SG621
Punc-25::RFP	This paper	SG622
Pacr-2(s)::RFP	This paper	SG623
Pflp-22::RFP	This paper	SG624
Pckr-1::GFP::unc-54-3′ UTR	This paper	SG124
Pckr-1::ckr-1::sl2dGFP	This paper	SG125
Pacr-2(s)::ckr-1::sl2dGFP	This paper	SG126
Pflp-22::ckr-1::sl2dGFP	This paper	SG228
Punc-47::ckr-1::sl2dGFP	This paper	SG182
Punc-25::ckr-1::sl2dGFP	This paper	SG225
Pnpr-9::ckr-1::sl2dGFP	This paper	SG231
Pglr-1::ckr-1::unc-54-3′ UTR-Pceh-63::gfp	This paper	SG208
Pzif-1(slot2)	This paper	SG235
Pckr-1::ZIF-1::sl2dGFP	This paper	SG243
Pinx-1::ZIF-1::sl2dGFP	This paper	SG244
Pflp-22::ZIF-1::sl2dGFP	This paper	SG247
Pglr-1::GCaMP6.0(s)::wCherry	This paper	SG133
Software and algorithms		
ImageJ	National Institutes of Health	https://imagej.nih.gov/ij/
Matlab	MathWorks	https://ww2.mathworks.cn/products/matlab.html
Clampfit	Molecular Devices	https://www.moleculardevices.com/p
Vector NTI	Thermo Fisher Scientific	https://www.thermofisher.cn/
GraphPad Prism 8	GraphPad Software Inc.	https://www.graphpad.com/
Igor Pro	WaveMetrics	https://www.wavemetrics.com/
MEGA 6.60	Molecular Evolutionary Genetics Analysis	https://megasoftware.net/

All data reported in this paper have been deposited at Mendeley Data (https://data.mendeley.com/preview/jm9yt2hdnk).

RESOURCE AVAILABILITY

Lead contact

Further information and requests for resources and reagents should be directed to and will be fulfilled by the lead contact, Shangbang Gao (sgao@hust.edu.cn).

Materials availability

- Plasmids generated in this study have been deposited to unique identifier (SG##).
- Worm lines generated in this study have been deposited to unique identifier (SGA##).
- This study did not generate new unique reagents.

Data and code availability

All data reported in this paper have been deposited at Mendeley Data and are publicly available as of the date of publication (https://data.mendeley.com/preview/jm9yt2hdnk).

This paper does not report the original code. Any additional information required to reanalyze the data reported in this paper is available from the lead contact upon request.

EXPERIMENTAL MODEL AND STUDY PARTICIPANT DETAILS

Worm maintenance and strains

All *C. elegans* strains were cultured on the standard Nematode Growth Medium (NGM) plates seeded with OP50 and maintained at 22°C. For experimentation, hermaphrodites at either the L4 stage or in the young adult phase (24 h post-L4 stage) were used. *In situ* electrophysiology experiment, 1- or 2-day-old hermaphrodite adults were used.

The wild type animal refers to the Bristol N2 strain. All mutants were sourced from the *Caenorhabditis Genetics Center* (*CGC*) and *National Bioresource Project (NBRP)*. The generation of transgenic strains (*gaaEx*) involved the injection of plasmid DNA. Integrated transgenic strains (*gaaIs*) were generated from the *gaaEx* animals by UV irradiation, followed by outcrossing against N2 at least 4 times before use. The complete lists of transgenic lines and strains generated or acquired for this study are provided in supplementary key resources table.

METHOD DETAILS

Molecular biology

The entry clone A slot1 was built using the In-Fusion method. All promoter fragments were amplified from N2 wild-type genomic lysates to substitute the "other promoter" fragment in standard BP reaction-generated entry clone A with the using ClonExpress One Step Cloning Kit (Vazyme, Nanjing). The length of P*nlp-12*, P*gpa*-4, P*ckr*-1, P*flp-22*, P*unc-25*, P*npr-9*, P*acr-2(s)* and P*inx-1* are 383 bp, 2470 bp, 1998 bp, 1532 bp, 1800 bp, 2000 bp, 3500 bp, and 898 bp, respectively.

All entry clone B slot2 and entry clones C slot3 were generated by using BP recombination reactions. The gene of interest, for example endogenous protein NLP-12, NLP-18 and CKR-1; exogenous functional proteins GCaMP6s, ChR2 and ZIF were combine into *pDONR221* vector as slot2. In generally, fluorescence protein or *unc-54*-3′UTR as target fragments were combine into *pDONR-P2R-P3* donor vector to generator slot3.

All expression constructs were generated with a Three-Fragment Multisite Gateway system (Invitrogen, Thermo Fisher Scientific, Waltham, MA, USA). Three entry clones A, B, C were recombined into the *pDEST R4-R3* Vector II or custom-modified destination vectors using attL-attR (LR) recombination reactions to generate expression clones. The complete lists of plasmid and vectors for this study are provided in supplementary key resources table.

Behavioral analyses

All the behavioral experiments were performed with young adult animals (12–18 h post L4 stage), maintained at 22 °C. The assay plates with layer of OP50 (6 cm nematode growth medium plates (NGM)) were prepared daily. Before the experiment, the OP50 lawn was spread evenly across the plate with a sterile bent glass rod. When all the preparation are ready, a single worm was gently picked onto assay plates with eyebrows. After a minute of acclimatization, a 3-min video of the spontaneous locomotion was recorded on a modified stereo microscope (Axio Zoom V16, Zeiss) with a digital camera (acA2500-60μm, Basler). All images were captured with a 10× objective at 10 Hz. To compare the data from different animals, the quantitative analysis of the behavioral parameters was performed using a custom-written script in MATLAB (MathWorks, Inc., Natick, MA) software. The central line was used to track. Images from each animal were divided into 32 body segments for curvature analysis. The curvatures at each point along the worm centerline *k(s)* can be calculated with the coordinate of each point *(x(s), y(s))* using the formula $k(s) = \frac{x'y'' x''y'}{(x'^2+y'^2)^{(3/2)}}$ where s is the normalized location along centerline (head = 0, tail = 1), and the unit of *k* is pixel^(−1). Then *k* is normalized with the length of worm body L, resulting in the dimensionless $k\sim(s)$ using the formula $\tilde{k}(s)=k(s)\times L$. The body curvature is the average value of 32 body segments. The Ω curvature means the average value of 0%–60% anterior part. In Figure 1, we separately analyzed the body curvature during forward and backward movements. Subsequently, the body curvature was analyzed primarily during forward movements (Figures 2, 4, and S1–S3).

In situ electrophysiology and calcium imaging

The dissection and recording procedures were conducted in accordance with protocols and solutions referenced from prior studies.[30,47,48] Briefly, 1- or 2-day-old hermaphrodite adults were glued (Histoacryl Blue, Braun, Germany) to a sylgard-coated cover glass covered with bath solution (Sylgard 184, Dowcorning, USA) under a DIC microscope. After clearing the viscera by suction through a glass pipette, the cuticle flap was turned and gently glued to the opposite side using WORMGLU (GluStitch Inc., Canada) to expose the neuromuscular system. Borosilicate pipettes (1B100F-4, World Precision Instruments, USA) were pulled by micropipette puller P-1000 (Sutter, USA), and fire-polished by microforge MF-830 (Narishige, Japan) into 4–6 MΩ. Minis and EPSCs were recorded from the body wall muscles in the whole-cell configuration holding at −60 mV by EPC9 amplifier (HEKA, Germany), by using the pulse and processed with Igor Pro (WaveMetrics, USA) and Clampfit 11 software (Molecular Devices, USA). Data were digitized at 10 kHz and filtered at 2.6 kHz. The pipette solution contains (in mM):

K-gluconate 115; KCl 25; $CaCl_2$ 0.1; $MgCl_2$ 5; BAPTA 1; HEPES 10; Na_2ATP 5; Na_2GTP 0.5; cAMP 0.5; cGMP 0.5, pH 7.2 with KOH, ~320 mOsm. cAMP and cGMP were included to maintain the activity and longevity of the preparation. The bath solution consists of (in mM): NaCl 150; KCl 5; $CaCl_2$ 5; $MgCl_2$ 1; glucose 10; sucrose 5; HEPES 15, pH 7.3 with NaOH, ~330 mOsm. Chemicals were obtained from Sigma unless stated otherwise. Light stimulation of *zxIs6* was performed with a LED light source at a wavelength of 460 ± 5 nm (3.75 mW/mm^2) to evoke post-synaptic currents. The light pulse was triggered by PULSE software with a duration of 10 ms. Experiments were performed at 22°C.

Follow the above dissection methods to expose SMD neuron for NLP-12 puffing evoked Ca^{2+} imaging. We monitored calcium transients in SMD neurons by the fluorescence intensity of the calcium indicator GCaMP6s. Then imaged with a 60× water objective (Nikon, Japan) and sCMOS digital camera (Hamamatsu ORCA-Flash 4.0 V2, Japan) at 10 Hz with expose time 100 ms. Throughout the SMD neuropeptide puffing experiments, the dissected nematode body was consistently exposed to extracellular fluid. Synthesized neuropeptides were dissolved in different concentrations of extracellular fluid. We recorded the neuronal Ca^{2+} transient by the perfusion of the NLP-12 neuropeptides for 60 s followed washing out for 50 s using normal bath solution. The Ca^{2+} transients of SMD soma were analyzed by Image-Pro Plus 6 (Media Cybernetics, Inc., Rockville, MD, USA). Then ratio change of SMD neuron Ca^{2+} signals was calculated using $\Delta F = (F - F_B)/F_B$. F_B means background signal.

Confocal fluorescence microscopy

Animals were anesthetized using an M9 salt solution containing 2.5 mM levamisole (Sigma-Aldrich) and mounted onto 2% agar pads. The animals were then visualized using a Plan-Apochromatic 60× objective on a confocal microscope (FV3000, Olympus). The fluorescence images were displayed and composited using ImageJ software (Wayne Rasband, National Institutes of Health, USA).

ZIF-1-ZF1 system

The ZIF-1-ZF1 system functions as an endogenous protein degradation mechanism, designed to rapidly eliminate specific proteins within targeted tissues and neurons in *C. elegans*.[33] This technique involves integrating sequences encoding the ZF1 tag into the endogenous loci, creating a modified strain with a specific target. Upon expression of the ZIF-1 E3 ubiquitin ligase substrate-recognition subunit in specific tissues and neurons, ZIF-1 recruits the ZF1-containing protein to an ECS E3 ligase complex for ubiquitination (Ub). Consequently, proteins labeled with the ZF1 zinc-finger domain undergo swift degradation across various somatic cell types.

Oocytes expression and two electrode voltage-clamp

CKR-1 expression in *X. laevis oocytes* was achieved through the following method: CKR-1 cDNAs were amplified and inserted between BamHI and HindIII sites using PCR. The resulting construct was cloned into the *pGH19* vector. CKR-1 cRNAs were generated using the mMessage Machine kit from Ambion. *X. laevis oocytes* were injected with 50 ng of CKR-1 receptor sense cRNAs. Injected oocytes were subsequently incubated at 18°C in the ND96 medium for 2–3 days prior to recording.

Current recordings were made using the two-electrode voltage-clamp technique at a holding potential of −80 mV.[49] Briefly, oocytes were continuously superfused with ND96 solution contains: 96 mM NaCl, 2.5 mM KCl, 1 mM $MgCl_2$ and 5 mM HEPES, pH 7.3. The recording chamber was perfused with high-K^+ solution to reverse the K^+ gradient[49] and measured the ligands dependent outward Ca^{2+}-gated chloride currents.[50] The pipette solution contains 3M KCl. The recording high-K^+ bath solution contains: 96 mM KCl, 2.5 mM NaCl, 1 mM $MgCl_2$ and 5 mM HEPES, pH 7.3. Peptide perfusion was terminated by washout with high-K^+ solution and subsequent switching to ND96 solution. Data were acquired with Clampex 8.0 software (Molecular Devices) and analyzed offline with Clampfit (Molecular Devices). Peptides were synthesized by the Guoping Pharmaceutical Company (Hefei, Anhui Province, China).

QUANTIFICATION AND STATISTICAL ANALYSIS

The Shapiro-Wilk test was used to check for normality and either Levene's test to check for equal variance. The two-tailed Student's *t*-test were used to compare normal distributed data from two groups, One-way analysis of variance (ANOVA) tested were used to compare data more than two groups. The Kolmogorov-Smirnov test is a non-parametric statistical test used to compare two samples and determine if they come from the same distribution. In this context, it is being used to analyze the shallow bending curvature cumulative fraction. $p < 0.05$ was considered to be statistically significant (*$p < 0.05$, **$p < 0.01$, ***$p < 0.001$). Graphing and subsequent analysis were performed using Igor Pro (WaveMetrics), Clampfit (Molecular Devices), ImageJ (National Institutes of Health), MATLAB (MathWorks), GraphPad Prism 8 (GraphPad Software Inc.), and Excel (Microsoft). For behavior analysis, electrophysiology and fluorescence imaging, unless specified otherwise, each recording trace was obtained from a different animal. Data were presented as the mean ± SEM.